Fachtagung "Experimentelle Strömungsmechanik"
6. – 8. September 2016, Cottbus

Komplementäre experimentelle und numerische Untersuchung der Strömung um eine starre und eine flexible Halbkugel in turbulenter Strömung: Teil I: Experimentelle Messungen

Complementary Experimental–Numerical Investigation of the Flow past a Rigid and a Flexible Hemisphere in Turbulent Flow: Part I: Experimental Measurements

J. N. Wood, M. Breuer
Professur für Strömungsmechanik, Helmut-Schmidt-Universität Hamburg, Germany.

Hemisphere; fluid-structure interaction; particle-image velocimetry; digital-image correlation; turbulent flow.
Halbkugel; Fluid-Struktur-Interaktion; Particle-Image-Velocimetry; Digital-Image Correlation; turbulente Strömung.

Abstract

This first part of a comprehensive experimental and numerical study investigates the fluid-structure interaction of a wall-mounted flexible hemisphere exposed to a turbulent boundary layer. The Reynolds number of the air flow is set to Re = $\rho_{air}\, U_\infty\, D\, /\, \mu_{air} \approx 50{,}000$, where D is the diameter of the hemisphere. The applied wind tunnel model of the hemisphere is made of silicone. It has to be pressurized to receive its hemispherical shape. The static and dynamic characteristics of the applied silicone (Young's modulus, damping coefficient) are evaluated by standardized tests. After this, the flexible hemisphere is transferred to the wind tunnel. The boundary conditions are set to match a previously conducted study in which the flow field of a rigid hemisphere was determined forming the base line of the present experiments. The flow measurements around the flexible hemisphere are carried out with particle-image velocimetry (PIV). In parallel the unsteady deformation of the structure due to the wind loads is captured by a high-speed three-dimensional digital-image correlation (DIC) system. The velocity field in combination with the frequency spectra of the structure oscillations are used to identify interactions of the flexible membrane with the wind loads. Supplementary pressure measurements are conducted in order to maintain stable conditions. All three measurement principles (PIV, DIC and pressure measurements) are combined to characterize the fluid-structure interaction problem of the flexible hemisphere.

Introduction

In modern civil engineering thin flexible structures are essential elements for present and future buildings. Weight reduction and optimized space utilization are major objectives to enhance environmental standards. These requirements are often satisfied by membranous structures that feature a cost-efficient solution for a fast construction of large span elements. Typical concepts for membranes used as main structural components are tents, facades or air-inflated structures. According to these applications, the incorporation of membranous elements raise important design issues that have to be considered carefully. A major challenge in urban environments is the response of the flexible structure to wind loads. Critical flow ve-

Karlsruhe, Germany, ISBN 978-3-9816764-2-6

locities or temporal gusts can trigger structural instabilities due to high static compression loads or dynamic response phenomena such as vortex or movement induced excitations (MIE) described by Naudascher and Rockwell (1994). This leads to the motivation for the present study. The topic of fluid-structure interaction of membranous structures under wind loads is of high relevance in a variety of applications. At present, there are only a few detailed experimental cases available in the literature, which take both the fluid and the structure side equivalently into account. Since such a data basis is highly desirable for a better physical understanding but also for the validation purposes of developed FSI simulation methodologies, the present study contributes to fill this gap. For this purpose, experimental investigations focus on a thin-walled air-inflated membranous structure in the shape of a hemisphere. This geometrically simple hemispherical dome is considered to be exposed to a thick turbulent boundary layer and thus the geometry and the operating conditions are clearly defined. The experimental investigations are conducted in a subsonic wind tunnel including both comprehensive particle-image velocimetry (PIV) for measuring the flow field and digital-image correlation (DIC) measurements of the structural deformations. That allows to characterize the fluid-structure interaction between the deformable structure and the flow field. In order to maintain the hemispherical shape, a small gauge pressure inside the model has to be brought up. To identify the characteristics of the FSI phenomenon, the results are compared with the flow field investigations of a rigid hemisphere at a Reynolds number of Re = 50,000 that are carried out under identical boundary conditions in Wood et al. (2016) and http://qnet-ercoftac.cfms.org.uk/w/index.php/UFR_3-13. Characteristics of the flow field and the response of the flexible structure are brought into correlation to analyze the complete fluid-structure interaction phenomenon.

Test Case Description

Figure 1 depicts the investigated case of a flexible hemisphere (diameter D) mounted on a smooth surface. The air-inflated structure is exposed to a turbulent flow (ρ_{air} = 1.225 kg/m^3, μ_{air} = 18.27 x 10^{-6} kg/(m s)) which corresponds to a Reynolds number of Re = $\rho_{air} U_\infty D / \mu_{air} \approx$ 50,000. U_∞ is the mean free-stream velocity in x-direction outside the boundary layer and is equal to 5.14 m/s. The turbulent flow describes a thick turbulent boundary layer. This wall-bounded flow follows a 1/7 power law in the boundary layer. The thickness of the boundary layer δ corresponds to the height of the hemisphere, i.e., $\delta = D/2$. The pressure difference, which is necessary to keep the hemisphere in shape, is $\Delta p_{FSI} = p - p_\infty$ = 19 Pa. The wall thickness of the flexible hemisphere correspond to $t_{membrane}$ = 0.16 mm.

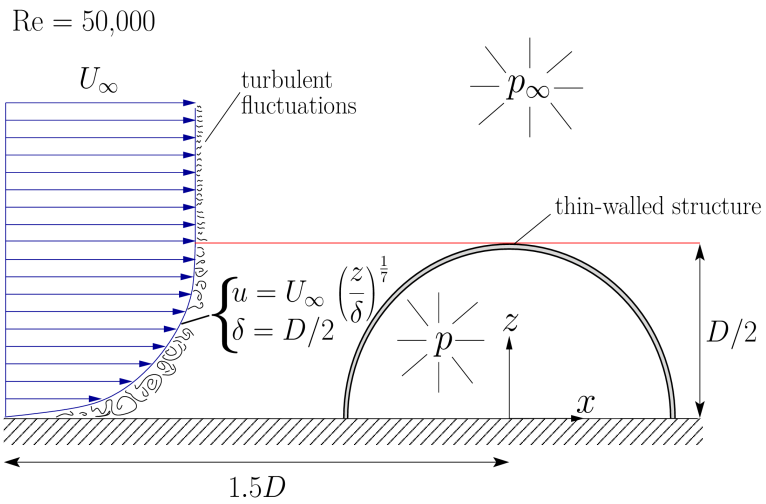

Fig. 1: Pressurized flexible hemisphere within a turbulent boundary layer flow.

Experimental Setup

The experimental investigations for the fluid-structure interaction of the flexible hemisphere are conducted in a Göttingen-type subsonic wind tunnel with an open test section. To achieve a fully developed turbulent boundary layer at the inlet of the test section according to predefined inflow conditions, customized vortex generator are placed inside the nozzle. The velocity profile of the artificially generated turbulent boundary layer corresponds well to the universal 1/7 power law. A detailed description of the design specifications of the vortex generators and the properties of the boundary layer can be found in Wood et al. (2016). That includes the distribution of the time-averaged mean velocity profile as well as the corresponding profiles of the Reynolds stresses.
The study on the FSI of the flexible hemisphere requires a suitable model. Two major aspects are considered during the manufacture of the model: First, the wall thickness $t_{membrane}$ has to be thin enough to approximate the two-dimensional character of a membrane and to allow perceptible structural deformations under the considered wind load. Second, the size (diameter D) and the mean average surface roughness R_a should be comparable to the rigid model in order to allow a direct comparison with the rigid case. A casting process depicted in Fig. 2 is chosen to manufacture an adequate model. The corresponding casting mold is made of a positive and a negative hemispherical form. The contour of the negative shape is adjusted to the dimensions of the rigid hemisphere, i.e., $D = D_{neg} = 150$ mm, to ensure geometrical identity between the flexible and the rigid model. The positive form is set to a diameter of $D_{pos} = 149.6$ mm so that a gap of approximately 0.2 mm between both shapes arises, which corresponds to the wall thickness $t_{membrane}$ of the flexible model.

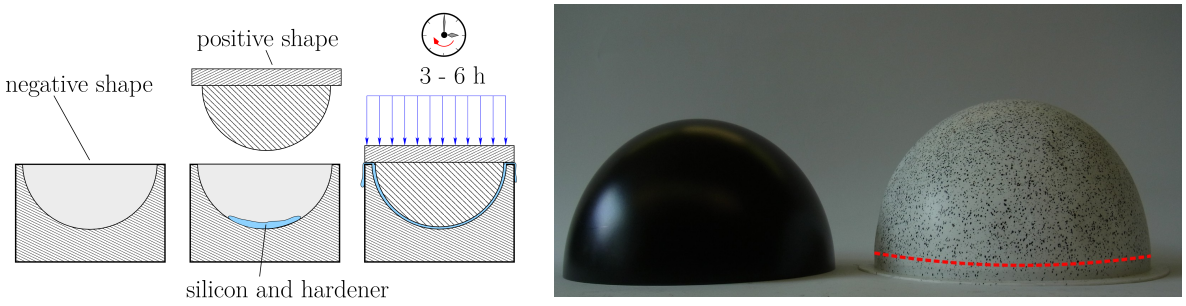

Fig. 2: Production of the flexible model. Rigid (left) and flexible (right) model of the hemisphere.

The overall size of the flexible model is identical to the rigid hemisphere. Additionally, the flexible model has a cylindrical extension with a pedestal foot for the connection to the flat plate which is placed into the test section of the wind tunnel. The separation between the hemispherical shape and the additional part is indicated in Fig. 2 by the red dashed line. The latter is enwrapped into the flat plate.

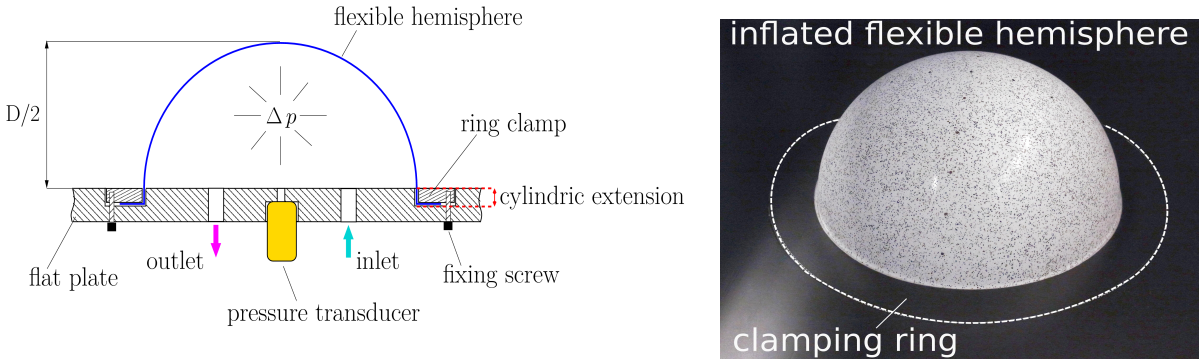

Fig. 3: Connection of the flexible hemisphere and the flat plate in the wind tunnel setup.

A schematic illustration of the connection between the model and the flat plate is depicted in Fig. 3 (left). The cylindrical extension of the hemisphere is put into a circular ring cutting that is inserted into the flat plate. A corresponding clamping ring is placed into the cutting and presses onto the pedestal of the model. The connection is fixed by stud hole screws. To maintain an even surface of the flat plate, the height of the ring can be adjusted by the screws on the lower side. Furthermore, air inlet and outlet drillings ensure a nearly constant pressurization inside the hemisphere in order to avoid air-leakage effects. The actual setup of the inflated model inside the test section of the wind tunnel is depicted in Fig. 3 (right).
The intended deformations of the flexible hemisphere during the wind tunnel test shall be mainly driven by the pressure difference between the outer surface of the membrane and the inner gauge pressure of the model as well as the shear stresses. Large quasi-static global deflections due to a large pressure difference between the environment and the interior of the model have to be avoided. Rather the membrane should be excited by the turbulent fluid flow. Consequently, the pre-stress originating from the pressure difference should be small and thus the inner pressure should be primarily used to stabilize the hemispherical shape. Thus, the operating pressure value to receive the desired deformations is evaluated experimentally. It leads to an ideal operating gauge pressure of Δp_{FSI} = 19 Pa. Below this value the inner pressure is not able to withstand the wind loads and large global deformations at the stagnation area in front of the hemisphere are observed.

Material Properties of the Applied Silicone

The material for the production of the flexible model is silicone Wacker Elastosil® E625 A/B RTV including a liquid component (A) in connection with a hardener component (B) in a mixture ratio of 9:1 (A:B). The properties of the applied silicone are determined by utilizing a standard tensile test (EN ISO 527-2) for the evaluation of the Young's modulus and a pendulum test (EN ISO 6721-2) for the measurement of the damping ratio of the applied material. The Young's modulus is estimated by linearizing the stress-strain correlation of the tensile test in the specific region $0 \leq \varepsilon \leq 0.1$ to $E_{silicone} \approx 700{,}000$ Pa. It is assumed that the material strain during the wind tunnel test is within this range due to the moderate wind loads that act on the surface of the flexible hemisphere. A Lehr damping factor of $b \approx 5\%$ of the material was evaluated by analyzing the decay of the measured oscillations. The corresponding measurements of the tensile test (left) and the pendulum test (right) are presented in Fig. 4.

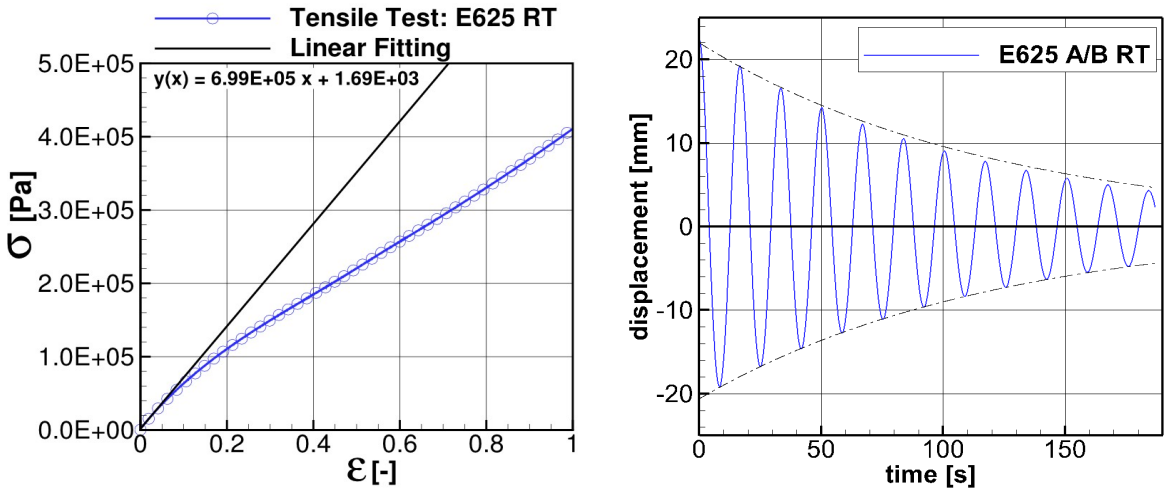

Fig. 4: Evaluation of the material properties of the chosen silicone material.

Measurement Techniques for the Fluid-Structure Interaction

To measure the FSI of the flexible hemisphere in turbulent flow, three independent measuring techniques are used: Particle-image velocimetry for the flow field in the symmetry plane, digital-image correlation for the deformation measurement of the membrane structure and a pressure transducer to record the pressure difference between the interior of the hemisphere and the environment. The flow field and the deformation measurements are conducted independently, since the applied standard mono PIV method has a significantly lower sampling rate of 15 frames per second (fps) compared to the high-speed cameras used for the deformation measurement (250 fps). Furthermore, the necessity of a constant high-energy light source for the DIC method makes it difficult to measure the flow field at the same time, since the powerful illumination overexposes the PIV images. Both setups are schematically presented in Fig. 5. The mono PIV setup (left) uses a Nd YAG laser with maximum energy of 200 mJ. The light sheet is reflected by an adjustable mirror which is set to the symmetry plane of the hemisphere. A CCD camera records the flow field. The setup of the DIC (right) consists of two high-speed cameras. The stereoscopic view and a speckle pattern on the surface of the hemispherical model are necessary to receive three-dimensional information about the unsteady structural deformations of the flexible structure. A pressure transducer records the pressure difference of the flexible hemisphere with a sampling rate of 200 Hz.

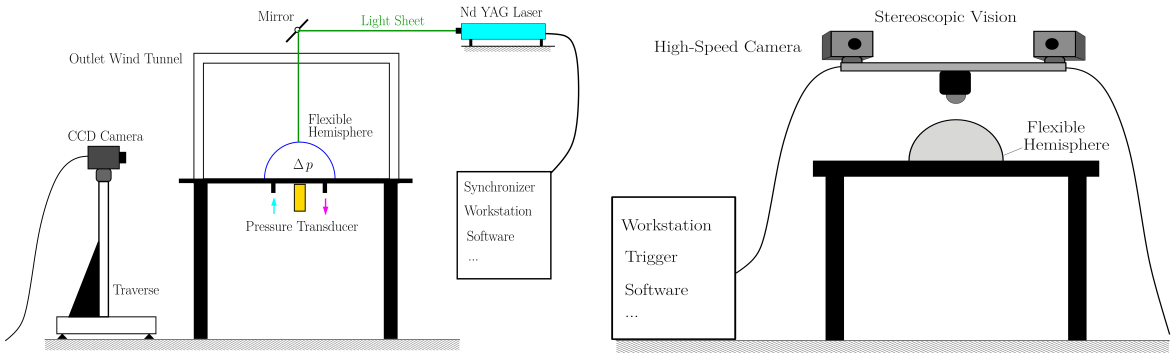

Fig. 5: Setup of particle-image velocimetry (PIV) and digital-image correlation (DIC) measurements.

Results

A comparison between the time-averaged flow field past the rigid and the flexible hemisphere in the symmetry plane is depicted in Fig. 6. The presented velocity profiles in the direct vicinity of the hemisphere show significant deviations. Obviously, oscillations of the flexible structure influence the flow field, especially visible in the wake regime at x/D = 0.4 for the wall-normal component $\overline{w}/U$. A first assumption is that the deflections of the flexible structure lead to smaller a recirculation area similar to the observations from Rojratsirikul et al. (2009, 2010)

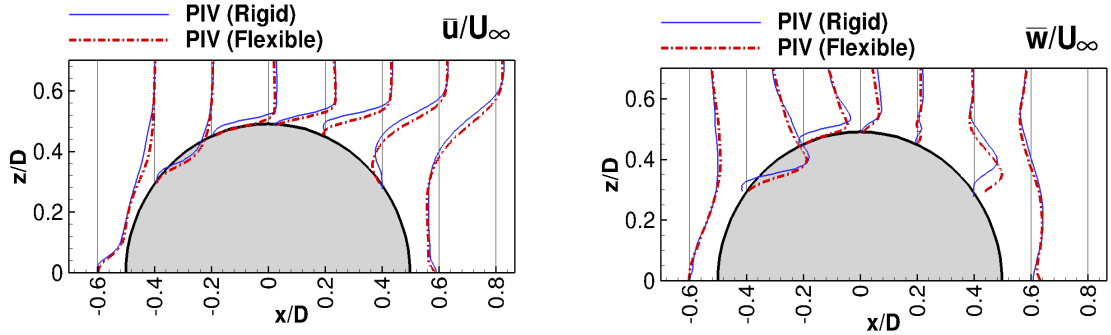

Fig. 6: Comparison of the time-averaged flow field past the rigid and the flexible hemisphere.

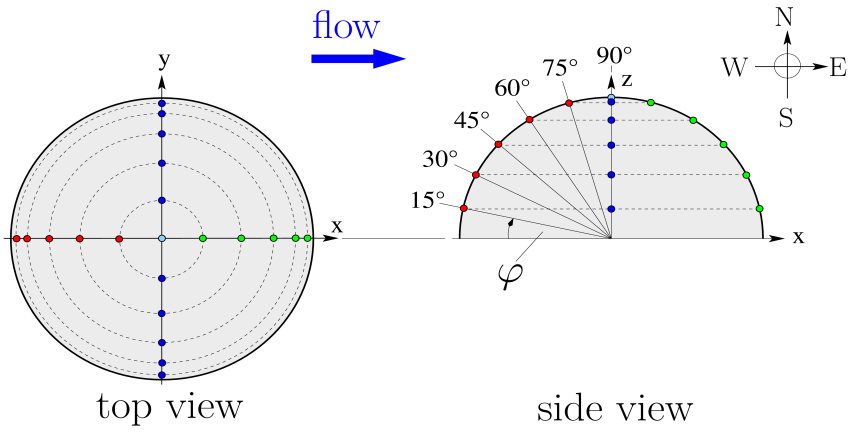

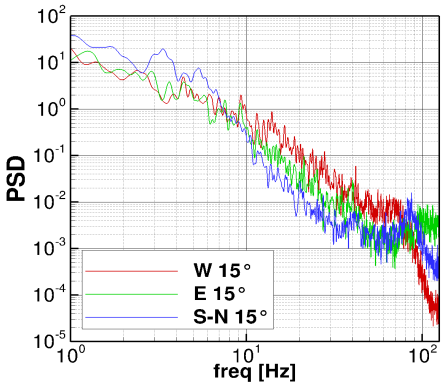

(a) Monitoring points at φ = 15°.

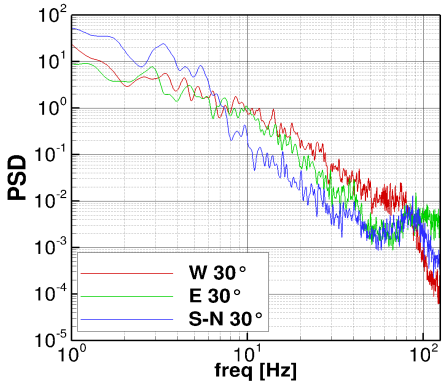

(b) Monitoring points at φ = 30°.

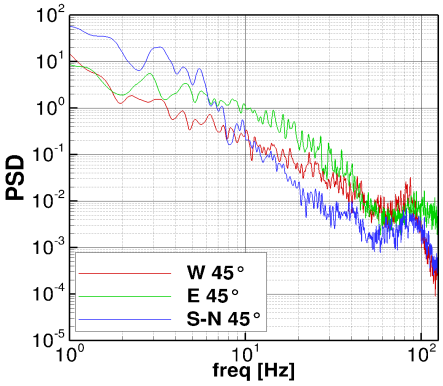

(c) Monitoring points at φ = 45°.

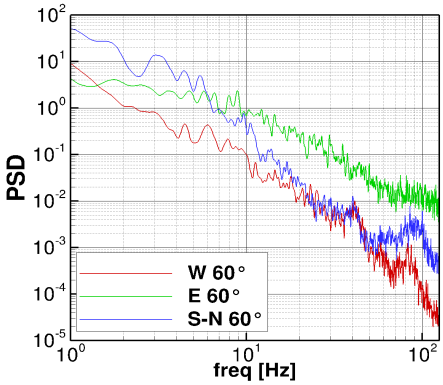

(d) Monitoring points at φ = 60°.

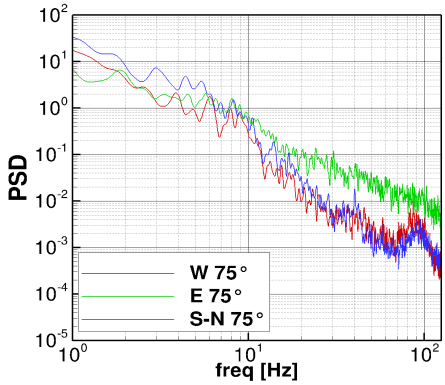

(e) Monitoring points at φ =75°.

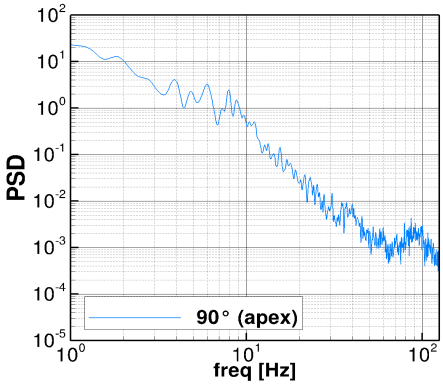

(f) Monitoring point at φ =90° (apex).

Fig. 7: Spectra of the dynamic response of the flexible structure to the wind load.

in case of a flexible membrane airfoil. Nevertheless, further PIV measurements with a high-spatial resolution camera are planned to highlight this phenomenon in more detail.
A DIC measurement was conducted to characterize the dynamic structural response of the flexible hemisphere due to the fluid loads of the turbulent flow regime. During the experiment the high-speed camera system is set to a sampling rate of 250 fps. This setting ensures a time-independent data sample of the deformation characteristics of the flexible structure. The memory of the camera allows to collect data in a time span of 22.5 seconds at the selected frame rate with a resolution of 1502 x 996 pixels.
The results of this campaign are presented in Fig. 7. The top and side view of the hemisphere illustrates schematically the location of the chosen monitoring points of the DIC measurements. All together there are 21 monitoring points on the surface of the flexible hemisphere. These are transferred to a simple compass system: west (front-side), east (wake-side), north and south (lateral sides). The flow direction is from east to west. From the origin of the initial coordinate system (center of the base area of the hemisphere) the points are mapped onto the surface by the angles φ = {15°,30°,45°,60°,75°} referring to each compass direction. The point at the apex of the hemisphere is defined at φ = 90°. The points on the south and north axes are considered to be comparable in their general deformation behavior due to the symmetry of the hemisphere. In fact the results of these points showed a nearly identical specturm during the measurements. Therefore, both are combined in the diagrams. Figures 7(a) – (f) present the frequency spectra of the oscillations of the membrane deflection due to the turbulent flow. The spectra are presented as power spectral density (PSD) plots that are generated from the total displacement $\Delta r = \sqrt{\Delta x^2 + \Delta y^2 + \Delta z^2}$ at each monitoring point. The PSD defines the power content of the displacement signal of the measured structural oscillations. Dominant frequencies in the spectrum have a higher power magnitude and can be connected to a particular excitation effect such as a movement or vortex induced vibrations (Naudascher and Rockwell, 1994). Every diagram depicts the dynamic response of the structure at each compass location (west, east, south-north) at a fixed angle φ in the frequency range 1 Hz ≤ f ≤ 125 Hz. First, the front-side (west; red graph) of the monitoring points are discussed. At the angles φ = 15° and φ = 30° (Fig. 7 (a) and (b)) the monitoring points exhibit a larger power magnitude throughout a major part of the measured frequency range. This effect is connected to a high pressure region on the surface at the front-side of the hemisphere due to the forming stagnation area which leads to large deflections. This area is also affected by the horseshoe vortex that curls around the front of the hemisphere. Dominant frequencies in the range 9.5 Hz ≤ f ≤ 15 Hz are present. Moving towards the apex of the hemisphere the amplitudes of the power spectrum decrease and two frequencies f = 41 Hz and 84 Hz remain visible. These oscillations can be linked to resonance effects of the flexible hemisphere that are triggered by the wind loads. They correspond to the eigenfrequencies of the membranous structure found in a preliminary study without fluid flow, where the pressurized structure was excited by a loud speaker in a predefined frequency range. Shifting to the wake-side (east; green graph) of the hemispherical dome, a significantly different oscillation behavior can be found. It seems that the highly turbulent wake regime, associated to the recirculation area, excites the flexible membrane at higher frequencies. Again, this is visible for the angles φ = 15° and φ = 30° (Fig. 7 (a) and (b)) where large power magnitudes at higher frequencies in the range 70 Hz ≤ f ≤ 125 Hz are found. Of special interest is the development in downstream direction visible in Fig. 7 (d) and (e). Here the magnitudes of the power spectra are much larger compared to the other locations (west, south-north) at these angles. This region is dominated by the roll-up effect of the shear layer where large coherent vortex structures detach from the separation line and are transported downstream. The lateral side (south-north; blue graph) shows large amplitudes at a lower frequency range between 3 Hz ≤ f ≤ 6 Hz compared to its overall spectrum. These frequencies can be explained by a quasi-periodic von Kármán vortex shedding pro-

Karlsruhe, Germany, ISBN 978-3-9816764-2-6

cess that is also observed in case of the rigid hemisphere (Manhart, 1998 and Wood et al., 2016). Additionally, two frequency peaks are detected at f = 41 Hz and 90 Hz at all points which indicate a resonance of the structure. The discussed diagrams present only a brief overview of the complex interaction between the fluid and the membranous structure. A connection between the structural oscillations measured by the DIC technique shall be combined with high-spatial resolution PIV measurements to determine the whole fluid-structure interaction problem of the flexible hemisphere in turbulent flow.

Conclusions

Experimental measurements of the fluid-structure interaction of an air-inflated flexible hemisphere were conducted in an open wind tunnel. The flow field and structure deformation were investigated at a Reynolds number of Re ≈ 50,000. To stabilize the thin-walled silicone model a pressure difference of Δp_{FSI} = 19 Pa is applied. Before the actual test could start, the material properties of the utilized silicone (Elastosil® E625 A/B RT) had to be evaluated. A standard tensile test was used to estimate the elastic behavior. Additionally, a pendulum test was applied to characterize the damping of the material. Afterwards, the comparison of the flow field around the rigid and the flexible model was analyzed using the particle-image velocimetry. The time-averaged flow field showed significant differences of the investigated velocity profiles between both cases, especially in the wake regime. At present, further PIV experiments with a higher spatial resolution are conducted to gain more insight into this phenomenon in order to clarify this effect. The second experiment focused on the dynamic response of the structure to the wind loads. The power magnitude and the frequency spectra of the displacement signals at chosen monitoring points on the surface of the flexible structure revealed a complex oscillation behavior. Dominant frequencies of the structure deflection could be connected to specific flow regimes, such as the stagnation area in front of the hemisphere. The wake regime showed large deformations at higher frequencies that are assumed to be caused by strong turbulent fluctuations in the recirculation area. Lower frequencies in the range between 3 Hz ≤ f ≤ 6 Hz at the lateral sides of the hemispherical dome are associated with a quasi-periodic von Kármán vortex shedding process. This was also seen in case of the rigid hemisphere. Nevertheless, more investigations of the flexible hemisphere are still needed to determine the whole fluid-structure interaction. In parallel, complementary numerical simulations (see **part II** of this paper) are carried out on the basis of the experimental case. An experimentally validated FSI algorithm offers the advantage of high spatio-temporal and fully three-dimensional simulations that go beyond the limits of the present measurement equipment.

References

ISO 527-2:2012: “Plastics – Determination of tensile properties – Part 2: Test conditions for moulding and extrusion plastics”.
ISO 6721-2:2008: “Plastics – Determination of dymanic mechanical properties – Part 2: Torsion-pendulum method”.
Manhart, **M**., 1998: “Vortex shedding from a hemisphere in a turbulent boundary layer”, Theoretical Computational Fluid Dynamics 12:1-28.
Naudascher, **E**., **Rockwell**, **D**., 1994: “Flow-induced Vibrations: An Engineering Guide”, AA Balkema, Rotterdam, Holland.
Rojratsirikul, **R**., **Wang**, **Z**., **Gursul**, **I**., 2009: “Unsteady fluid-structure interactions of membrane airfoils at low Reynolds numbers”, Experiments in Fluids 46:859-872.
Rojratsirikul, **R**., **Wang**, **Z**., **Gursul**, **I**., 2010: “Effects of pre-strain and excess length on unsteady fluid-structure interactions of membrane airfoils”, Journal of Fluids and Structures 26:359-376.
Wood, **J**.**N**., **De Nayer**, **G**., **Schmidt**, **S**., **Breuer**, **M**., 2016: “Experimental investigations and large-eddy simulation of the turbulent flow past a smooth and rigid hemisphere”, Flow, Turbulence and Combustion 97:97-119.

Karlsruhe, Germany, ISBN 978-3-9816764-2-6